

## Synchronized states in a ring of dissipatively coupled harmonic oscillators

Juan N. Moreno <sup>1,\*</sup>, Christopher W. Wächtler <sup>1,2,†</sup> and Alexander Eisfeld<sup>1,3,‡</sup>

<sup>1</sup>Max Planck Institut für Physik komplexer Systeme, 01187 Dresden, Germany

<sup>2</sup>Department of Physics, University of California, Berkeley, California 94720, USA

<sup>3</sup>Universität Potsdam, Institut für Physik und Astronomie, 14476 Potsdam, Deutschland

 (Received 30 January 2023; revised 3 August 2023; accepted 15 December 2023; published 23 January 2024)

The question under which conditions oscillators with slightly different frequencies synchronize appears in various settings. We consider the case of a finite number of harmonic oscillators arranged on a ring, with bilinear, dissipative nearest-neighbor coupling. We show that by tuning the gain and loss appropriately, stable synchronized dynamics may be achieved. These findings are interpreted using the complex eigenvalues and eigenvectors of the non-Hermitian matrix describing the dynamics of the system. We provide a complete discussion for the case of two oscillators. Ring sizes with a small number of oscillators are discussed taking the case of  $N = 5$  oscillators as an example. For  $N \gtrsim 10$  we focus on the case where the frequency fluctuations of each oscillator are chosen from a Gaussian distribution with zero mean and standard deviation  $\sigma$ . We derive a scaling law for the largest standard deviation  $\sigma_{\text{full}}$  that still permits all oscillators to be fully synchronized:  $\sigma_{\text{full}} \sim N^{-3/2}$ . Finally, we discuss how such random fluctuations influence the timescale on which the synchronized state is reached and on which timescale the synchronized state then decays.

DOI: [10.1103/PhysRevE.109.014308](https://doi.org/10.1103/PhysRevE.109.014308)

### I. INTRODUCTION

Synchronization is a fascinating phenomenon that can be interpreted as a display of cooperative behavior appearing in many complex systems [1,2]. Since the first observation by Huygens in the late 1600s [3], it has been studied in diverse communities, where it plays an important role in our understanding for example in electric networks in engineering, circadian rhythms in biology, pattern formation in statistical mechanics, and chemical reactions in chemistry [4–6]. Other examples are laser networks [7], phase-locked loops [8], Josephson junction arrays [9,10], spin-torque resonators [11], power grids [12], and communication networks [13,14].

Typically synchronization is investigated in the context of the adjustment of rhythms of autonomous oscillators, which attain stable periodic orbits without active regulation from the outside [15] and thus require nonlinearities in the governing equations of motion. Far less common is the investigation of synchronization in models that are linear in both the oscillators and the couplings. Although linear systems are in general well understood, the specifics of the considered network topology may facilitate different dynamical features, in particular with regards to synchronization. Such linear models

appear for example after certain transformations of the Kuramoto model [16], in the context of feedback control theory [17,18] or in the description of coupled electronic LC circuits [19–21]. Many photonic systems can also be well described by a model of linearly coupled harmonic oscillators, such as coupled cavities [22] or waveguides [23,24]. Furthermore, linearly coupled oscillators emerge when mapping quantum dynamics to classical representation [25].

Without dissipation, coupled harmonic oscillators form collective eigenmodes, where the individual oscillators perform motion with a fixed phase relation [26,27]. However, a system not initialized in an eigenmode usually stays in a superposition of several eigenmodes with different eigenfrequencies resulting in a beating pattern. Moreover, if the number of coupled oscillators is large, then the system dynamics does not need to exhibit perfect revivals in general [28] and synchronized motion is absent. Hence in a closed system of oscillators, only for an eigenmode as the initial condition does one obtain a time-independent phase relation between the oscillators. However, if the system is not closed, but subject to gain and loss, then the open system dynamics allow for a situation where all eigenmodes but one are damped. Then, synchronization is possible as long as the respective eigenstate is present in the initial state. However, in order to achieve a situation where all but one mode are damped, one needs to carefully balance gain and loss.

In contrast to a self-sustained system where the nonlinearity counteracts the dissipation (or gain) in order to stabilize periodic orbits, a *single* linear harmonic oscillator only exhibits the following dynamics in the absence of periodic driving: Either the dissipation exceeds the gain, such that the amplitude of the dissipative systems shrinks and eventually reaches a single point in phase space, or in the other way around, where the gain exceeds the dissipation, the oscillation

\*moreno@pks.mpg.de

†cwwaechtler@berkeley.edu

‡eisfeld@pks.mpg.de

amplitude infinitely grows. In the special case where both are equivalent the system is effectively described by closed system dynamics with infinitely many closed orbits in phase space depending on the initial energy of system. However, when coupling between linear oscillators are introduced, more solutions are possible [29]. In the context of synchronization, non-Hermitian linearly coupled oscillators have been investigated in various arrangements and with various aims (see, e.g., Ref. [30]).

Here we investigate a ring-network of linear harmonic oscillators subject to gain and loss and focus on the case when the coupling between the oscillators is purely dissipative [31]. Such dissipative coupling has been studied both for linear [32–36] and nonlinear [37–39] systems. The simultaneous presence of gain and loss allows for the emergence of dissipation-free subspaces in parameter space. Within these subspaces we find periodic motion of all oscillators in the network that is starting from an (nearly) arbitrary initial state the system reaches a regime during time propagation in which all oscillators exhibit synchronized motion for a long time. At this point, let us specify the notion of synchronization we use throughout this work:

(1) With “long time” we mean times long compared to the eigenfrequencies of the individual oscillators and we focus on the case where all oscillators have small deviations from a common “mean frequency.” In the ideal case they oscillate forever.

(2) With “synchronized” we mean that the oscillators have a fixed phase relation. Ideally, we want that all oscillators have the same amplitude. If this is the case, then we denote it as *full synchronization*. If the system is not in a fully synchronized state, then we will characterize its *degree of synchronization* by a suitable measure.

(3) With “arbitrary” initial state we mean that for most initial states synchronization is achieved, yet there exist some special initial conditions that do not lead to synchronization.

We note that within the above definitions for uncoupled oscillators, one only finds synchronization when there is no gain and loss and all oscillators have the same frequency. We emphasize that we are not particularly interested in the thermodynamic limit where the number of oscillators goes to infinity but in the dynamics for a finite number of oscillators.

The remainder of the paper is organized as follows: In Sec. II A we summarize some general considerations of synchronization for linearly coupled harmonic oscillators important for our work, followed by the specific model under investigation in Sec. II B. In the subsequent Sec. III we discuss our results, which includes the special case of two coupled oscillators in Sec. III A and the more general case of many oscillators in Sec. III B. Finally, we conclude in Sec. IV.

## II. MODEL AND BASIC FORMALISM

### A. General considerations of synchronization in linear oscillator models

To introduce the basic concepts and notation, we consider  $N$  harmonic oscillators in a network, each labeled by a subscript  $n = 1, \dots, N$ . In the present work we are mainly interested in the regime  $N \lesssim 100$ , which could be implemented

via photonic setups [22,24]. It is convenient to describe the dynamics of the oscillators by dimensionless complex amplitudes. The equation of motion for an individual oscillator subject to dissipation is given by  $\dot{a}_n(t) = (-i\Omega_n - \gamma)a_n(t)$ . Its solution  $a_n(t) = a_n(0) \exp[(-i\Omega_n - \gamma)t]$  describes damped oscillatory motion with initial (complex) amplitude  $a_n(0)$ , frequency  $\Omega_n$ , and “damping”  $\gamma$ . Note that while for  $\gamma > 0$  the oscillator is indeed exponentially damped, for  $\gamma < 0$  (i.e., gain), the oscillator amplitude grows exponentially (in an actual system one would have saturation effects which would have to be described by a nonlinear equation; therefore, we will consider only cases where the amplitudes of the oscillators do not grow exponentially). In the *coupled* system, the motional state of each oscillator is characterized by a time-dependent complex amplitude  $a_n(t) = |a_n(t)|e^{i\phi_n(t)}$ , which now, however, can deviate from the dynamics of the individual oscillator discussed above. If all oscillators in the network oscillate with a common real frequency  $\omega_{\text{syn}}$  while their relative amplitudes remain constant, then we will refer to it as synchronization. Using a vector notation  $\vec{a}(t) = (a_1(t), \dots, a_N(t))^T$ , such synchronized motion may be expressed as

$$\vec{a}(t) = f(t)\vec{a}_{\text{syn}}e^{-i\omega_{\text{syn}}t}, \quad (1)$$

where  $f(t)$  is a real function that takes into account the possibility that the amplitudes decay (or grow) over time, which we will discuss in Sec. II B in more detail. In the case of  $f(t) = 1$  the motion represents a periodic steady state, which we refer to as *ideal synchronized motion*.

The above notion is not sufficient to fully characterize synchronized motion as for example a single oscillatory site in the network (while all other oscillators are at rest) also fulfills Eq. (1). It is thus necessary to also quantify the *degree of synchronization* of a vector  $\vec{a}$ , which we denote by  $\mathcal{S}(\vec{a})$ . To this end, we use the inverse participation ratio [40],

$$\mathcal{S}(\vec{a}) = \frac{1}{\sum_{n=1}^N |a_n|^4}, \quad (2)$$

which takes values between 1 and  $N$ . Here a value of  $\mathcal{S} = 1$  corresponds to the aforementioned case of a single oscillator in motion, whereas a value of  $\mathcal{S} = N$  indicates *fully synchronized motion*, i.e., all nodes have the same absolute value of the amplitude. Values of  $\mathcal{S} = \tilde{N} < N$  correspond to *partial synchronization* of approximately  $\tilde{N}$  oscillators. In Fig. 1, we illustrate different degrees of synchronization and their respective dynamics in a network of three oscillators.

The time evolution of a linearly coupled network of harmonic oscillators in the presence of gain and loss is expressed as

$$\frac{d}{dt}\vec{a} = W\vec{a}, \quad (3)$$

where we assume the non-Hermitian matrix  $W$  to be time independent. The diagonal elements contain the frequencies of the individual oscillators and their loss or gain, as described above. The off-diagonal elements  $W_{nm}$  are the couplings between the oscillators  $n$  and  $m$ . In components this reads  $\dot{a}_n = \sum_m W_{nm}a_m$ . From this equation one clearly sees that for *complex*  $W_{nm}$  the real and imaginary parts of oscillator  $n$  become coupled to both the real and imaginary parts of the

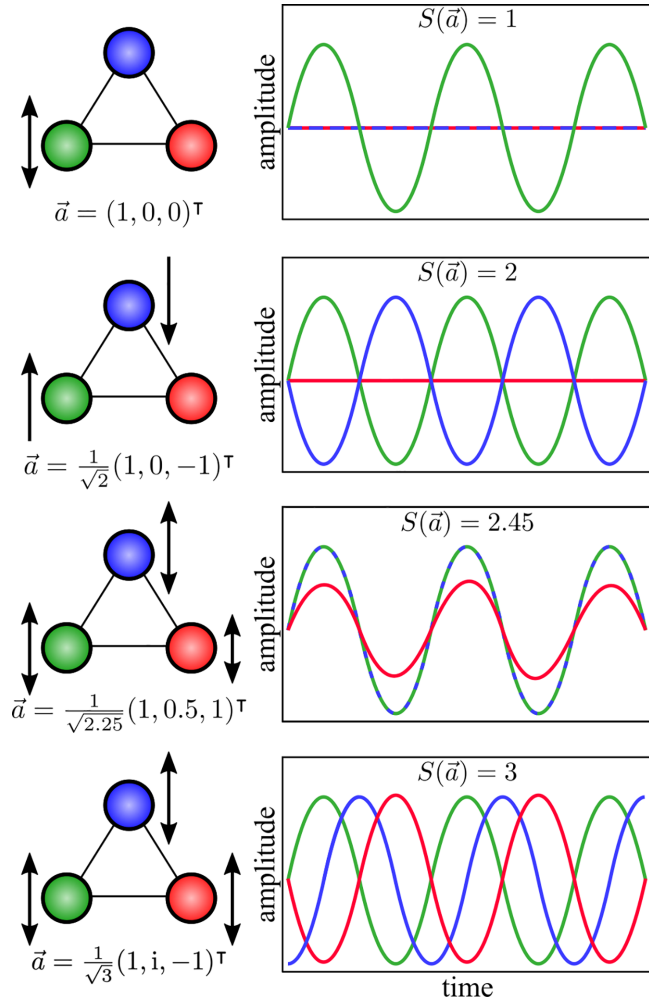


FIG. 1. Illustration of potentially attainable synchronized motion in a network of  $N = 3$  oscillators. The inverse participation ratio  $S(\vec{a})$  increases from top to bottom in accordance with the transition from partially to fully synchronized motion.

oscillator  $m$ . In Appendix A we provide the form of this equation for real and imaginary parts separately and also for the representation  $a_n = |a_n|e^{i\phi_n}$  with real amplitude  $|a_n|$  and real phase  $\phi_n$ . The state of the system at time  $t$  is given by the formal solution

$$\vec{a}(t) = e^{Wt}\vec{a}(0), \quad (4)$$

where  $\vec{a}(0)$  denotes the initial state at time  $t = 0$ . Thus, the dynamics of the network is fully characterized by the matrix  $W$ , in particular by its eigenvalues and eigenvectors. For some special cases, the matrix  $W$  can be diagonalized analytically (see, e.g., Refs. [23,30,41]), but in general one has to perform the diagonalization numerically. Since  $W$  is (in general) non-Hermitian, one has to distinguish right and left eigenvectors defined via

$$W\vec{c}_j = w_j\vec{c}_j \quad \text{and} \quad \vec{z}_j^\dagger W = \vec{z}_j^\dagger w_j. \quad (5)$$

Here  $\dagger$  indicates the complex conjugated and transpose, and the eigenvectors are normalized according to

$$\vec{c}_j^\dagger \vec{c}_j = 1 \quad \text{and} \quad \vec{z}_j^\dagger \vec{c}_j = \delta_{j'j}. \quad (6)$$

Note that, in general,  $\vec{c}_j^\dagger \neq \vec{z}_j^\dagger$ . The matrix  $W$  can now be expressed as  $W = \sum_j w_j \vec{c}_j \vec{z}_j^\dagger$ , such that the time evolution of Eq. (4) is conveniently given by

$$\vec{a}(t) = \sum_j \vec{c}_j e^{w_j t} \vec{z}_j^\dagger \vec{a}(0), \quad (7)$$

where  $\vec{z}_j^\dagger \vec{a}(0)$  is the initial weight of the eigenstate  $j$ . While the imaginary part of the complex eigenvalue  $w_j$  determines the oscillation frequency of eigenmode  $j$ , the real part  $\text{Re}(w_j)$  determines whether the oscillatory motion is damped [ $\text{Re}(w_j) < 0$ ], growing [ $\text{Re}(w_j) > 0$ ], or oscillates forever [ $\text{Re}(w_j) = 0$ ].

In order to obtain a time evolution of the form of Eq. (1) with  $f(t) = 1$  after some initial transient time, i.e., dynamically reach the eigenstate with  $\text{Re}(w_{\text{sync}}) = 0$ , the initial state needs to have nonvanishing overlap with the synchronized eigenstate [ $\vec{z}_{\text{sync}}^\dagger \vec{a}(0) \neq 0$ ]. Furthermore, all other eigenstates present in the initial state need to have  $\text{Re}(w_j) < 0$ , such that they are damped. In the following, we will therefore search for conditions and parameters under which *one* eigenstate fulfills  $\text{Re}(w_{\text{sync}}) = 0$  while all other eigenstates fulfill  $\text{Re}(w_j) < 0$ . Subsequently, we will characterize the degree of synchronization of the resulting state in terms of  $S$ ; cf. Eq. (2).

## B. Linear oscillators with purely dissipative nearest-neighbor coupling

After the general considerations of the previous Sec. II A, let us now specify the network of interest throughout the remainder of this work: The individual oscillators have frequencies  $\Omega_n \in \mathbb{R}$  and are arranged on a ring. Each oscillator is subject to gain or loss mediated via the rate  $\gamma \in \mathbb{R}$  and interacts with its two nearest neighbors via a purely dissipative coupling  $v \in \mathbb{R}$ . For simplicity we assume that the coupling and dissipation is equal for all oscillators. We are interested in the possibility of synchronization when the frequency of each oscillator is different, which corresponds to the notion of synchronization as an adjustment of rhythms due to the presence of interactions. The equation of motion of the  $n$ th oscillator is then given by

$$\frac{d}{dt}a_n = (-i\Omega_n - \gamma)a_n - v(a_{n+1} + a_{n-1}), \quad (8)$$

with  $a_0 \equiv a_N$  and  $a_{N+1} \equiv a_1$  to fulfill periodic boundary conditions. Note that positive values of  $\gamma$  represent loss, whereas negative values correspond to gain. To simplify notation we express all energies in units of  $v$  and take  $v$  to be positive (the case of negative  $v$  will be discussed later), i.e.,  $\omega_n = \Omega_n/v$ ,  $g = \gamma/v$  and  $\tau = tv$ . Furthermore, we parametrize the frequencies as  $\omega_n = \bar{\omega} + \Delta_n$ . Then, Eq. (8) becomes

$$\frac{d}{d\tau}a_n = [-i(\bar{\omega} + \Delta_n) - g]a_n - (a_{n+1} + a_{n-1}). \quad (9)$$

Our goal in the following is to determine the values of  $g$  for a given set of frequency differences  $\Delta_n$ , such that the oscillators perform synchronized motion in the sense discussed in Sec. II A.

As the term  $(-i\bar{\omega} - g)$  is independent of the oscillator index  $n$ , it only trivially contributes to the overall dynamics; specifically oscillations with frequency  $\bar{\omega}$  and damping or

growing with rate  $g$ . In matrix representation, Eq. (9) can be written in the form of Eq. (3) with  $t \rightarrow \tau$  and  $W = (-i\bar{\omega} - g)\mathbb{I} + M$ , where

$$M = -i \begin{pmatrix} \Delta_1 & -i & 0 & \dots & -i \\ -i & \Delta_2 & -i & \dots & 0 \\ 0 & -i & & & \\ \vdots & & & & \\ -i & 0 & \dots & -i & \Delta_N \end{pmatrix}. \quad (10)$$

Note that the (left and right) eigenvectors of  $W$  and  $M$  are identical and their eigenvalues are simply shifted, i.e., if  $M\bar{c}_j = \lambda_j\bar{c}_j$ , then  $W\bar{c}_j = w_j\bar{c}_j$  with

$$w_j = -i[\bar{\omega} + \text{Im}(\lambda_j)] + [-g + \text{Re}(\lambda_j)], \quad v > 0. \quad (11)$$

Moreover, as  $M$  only depends on  $\Delta_n$ , the eigenvectors and thus the degree of synchronization  $\mathcal{S}(\bar{c})$  is independent of  $g$ .

Let us summarize as follows the general conditions of the previous Sec. II A for synchronized motion tailored to the specifics of our system discussed here:

(i) There exists a single eigenstate  $\bar{c}_{\text{sync}}$  of  $W$  with purely imaginary eigenvalue. This corresponds to a state  $\bar{c}_{\text{sync}}$  that fulfills  $-g + \text{Re}(\lambda_{\text{sync}}) = 0$ , where  $M\bar{c}_{\text{sync}} = \lambda_{\text{sync}}\bar{c}_{\text{sync}}$ .

(ii) All other eigenstates of  $W$  have negative real part for the set of parameters determined in (i). That corresponds to  $-g + \text{Re}(\lambda_j) < 0$  for all  $j \neq \text{sync}$ .

(iii) The synchronization measure  $\mathcal{S}(\bar{c}_{\text{sync}})$  should be as large as possible. Ideally  $\mathcal{S}(\bar{c}_{\text{sync}}) = N$ .

So far, we have taken  $v$  to be positive. For negative values of  $v$  we define the scaled energies in terms of  $-v$  such that  $\omega_n = \bar{\omega} + \Delta_n = -\Omega_n/v$ ,  $g = -\gamma_n/v$ , and  $\tau = -tv$ . Then, Eq. (9) becomes

$$\frac{d}{d\tau} a_n = [-i(\bar{\omega} + \Delta_n) - g]a_n + (a_{n+1} + a_{n-1}), \quad (12)$$

where the first term remains identical while the sign changes in front of the oscillator couplings, and thus the off-diagonal matrix elements of  $M$ , cf. Eq. (10). Here the imaginary part of the eigenvalues (as well as the corresponding eigenstates and the measure  $\mathcal{S}$ ) remains unchanged, while the real part simply changes its sign. Thus, eigenstates that are decaying for  $v > 0$  are growing for  $v < 0$  and vice versa.

### III. RESULTS

In the following, we first discuss the case of  $N = 2$  in Sec. III A, which provides a clear picture of the basic mechanism underlying the synchronization of linear oscillators interacting via dissipative couplings. Subsequently, we consider a ring of  $N > 2$  oscillators in Sec. III B and show that also in this case, synchronized motion may be achieved and follows similar arguments as before.

#### A. Two coupled oscillators ( $N = 2$ )

For two coupled oscillators, the problem reduces to analyzing a  $2 \times 2$  non-Hermitian matrix, for which the corresponding eigenvalue problem can be solved analytically. Similar matrices appear, e.g., for coupled ring resonators [42] or in the context of  $\mathcal{PT}$ -symmetric systems [43,44]. Here we provide the results for our system setup explicitly and discuss

their implications for synchronized dynamics. Without loss of generality, we may choose the scaled frequency differences of the two oscillators to be  $\Delta_1 = +\Delta$  and  $\Delta_2 = -\Delta$ , such that matrix  $M$  governing the dynamics [cf. Eq. (10)] is given by

$$M = -i \begin{pmatrix} \Delta & -i \\ -i & -\Delta \end{pmatrix}. \quad (13)$$

Here we have chosen  $v > 0$ . However, from the discussion in Sec. II B we know that a negative value of  $v$  simply results in a change of sign of the real part of the eigenvalues. The two eigenvalues and corresponding right eigenvectors of  $M$  are given by

$$\lambda_{\pm} = \mp i\sqrt{\Delta^2 - 1}, \quad (14)$$

$$\bar{c}_{\pm} = \frac{1}{\sqrt{1 + |\Delta \pm \sqrt{\Delta^2 - 1}|^2}} \begin{bmatrix} i(\Delta \pm \sqrt{\Delta^2 - 1}) \\ 1 \end{bmatrix}. \quad (15)$$

If  $|\Delta| < 1$  ( $|\Delta| > 1$ ), then the eigenvalues  $\lambda_{\pm}$  are both purely real (imaginary) and nondegenerate. In contrast, for  $\Delta = \pm 1$  not only are the eigenstates degenerate but also the corresponding eigenvectors coalesce, i.e., these values of  $\Delta$  correspond to exceptional points [45–48]. The impact of exceptional points on synchronization goes beyond the scope of the present work, and we will focus in the following on the cases  $|\Delta| > 1$  and  $|\Delta| < 1$ .

*a. Overview.* As discussed in Sec. II B, the eigenenergies  $w_{\pm} = -i[\bar{\omega} + \text{Im}(\lambda_{\pm})] + [-g + \text{Re}(\lambda_{\pm})]$  describe the overall possibility of long-lasting synchronized motion in terms of oscillation frequency and damping, while  $\mathcal{S}$  quantifies the degree of synchronization. Let us start by considering the real part of the eigenenergies  $w_{\pm}$  given by  $\text{Re}(w_{\pm}) = -g + \text{Re}(\lambda_{\pm})$ , which determines the (exponential) damping or growing. In Figs. 2(a) and 2(b) we show  $\text{Re}(w_-)$  and  $\text{Re}(w_+)$ , respectively, as a function of the frequency difference  $\Delta$  and the dissipation strength  $g$ . Note that  $\Delta$  as well as  $g$  can take on positive and negative values. The red areas in Figs. 2(a) and 2(b) indicate positive values corresponding to amplitude growth, whereas the blue areas indicate negative values and thus amplitude damping. Along the white separation between the two regions the amplitudes neither increase nor decrease. We discuss this most relevant line for dissipation-free synchronization in more detail below.

As expected from the discussion above, quite different behavior of  $\text{Re}(w_{\pm})$  is observed depending on whether  $|\Delta| > 1$  or  $|\Delta| < 1$ . Similarly, a pronounced difference is found in the behavior of the imaginary part  $\text{Im}(w_{\pm}) = -[\bar{\omega} + \text{Im}(\lambda_{\pm})]$ , which describes the oscillation frequency of the eigenmodes and is shown in Figs. 2(c) and 2(d). For  $|\Delta| < 1$  the frequency remains unchanged and both eigenstates oscillate with the mean frequency  $\bar{\omega}$ . However, for  $|\Delta| > 1$  the frequency of the  $-$  state [cf. Fig. 2(c)] is increasing, while that of the  $+$  state [cf. Fig. 2(d)] is decreasing. Both follow the functional form of a square root with opposite sign, cf. Eq. (14). Last, in Figs. 2(e) and 2(f) we show the degree of synchronization  $\mathcal{S}$  as function of  $\Delta$ , which is given by [cf. Eq. (15)]

$$\mathcal{S}(\bar{c}_{\pm}, \Delta) = \begin{cases} 2 & |\Delta| < 1 \\ 2\frac{\Delta^2}{2\Delta^2 - 1} & |\Delta| > 1. \end{cases} \quad (16)$$

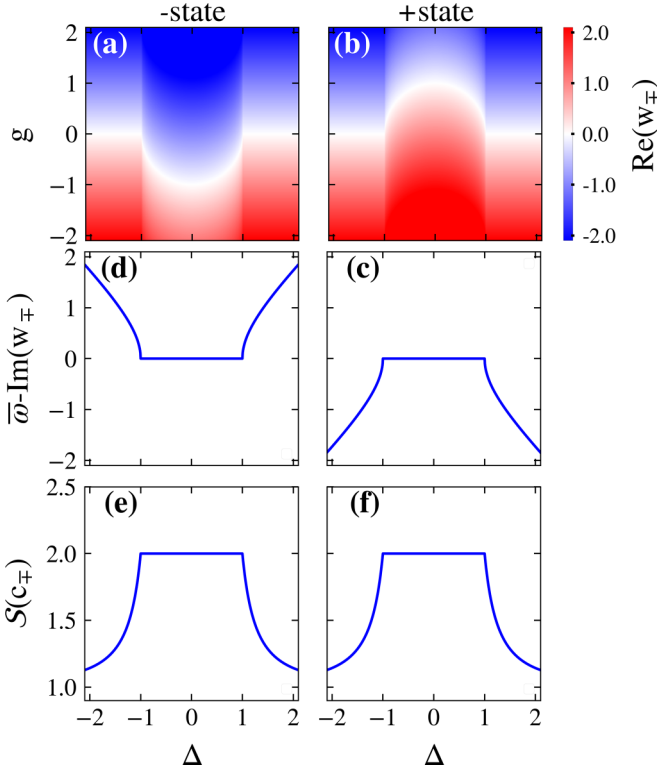


FIG. 2. Top row: Density plots of the real part  $\text{Re}(w_{\pm})$  as a function of the frequency difference  $\Delta$  and the dissipation strength  $g$ : (a)  $w_-$  and (b)  $w_+$ . Dissipation-free synchronization is found along the white line. Middle row: Corresponding imaginary part (c)  $\text{Re}(w_-)$  and (d)  $\text{Re}(w_+)$  as a function of  $\Delta$ , which corresponds to the oscillation frequency of the respective eigenvector. Last row: Degree of synchronization  $\mathcal{S}$  as function of  $\Delta$  of the eigenvalue (e)  $\bar{c}_-$  and (f)  $\bar{c}_+$ . The largest value is found for  $|\Delta| < 1$  corresponding to fully synchronized motion.

As expected, the maximum value lies within the range of  $|\Delta| < 1$  and rapidly decreases as  $|\Delta|$  increases, indicating the absence of synchronization. After this broad overview, we will discuss in more detail the potential of synchronized motion in the system of  $N = 2$  oscillators in the following, focusing on the three criteria (i)–(iii) formulated in Sec. II B.

*b. Detailed discussion of the regime  $|\Delta| > 1$ .* In this case, the eigenvalues  $\lambda_{\pm}$  become purely imaginary [cf. Eq. (14)], such that the eigenenergies take the simple form  $w_{\pm} = -i(\bar{\omega} \pm \sqrt{\Delta^2 - 1}) - g$ . Most importantly, the real part is solely given by  $-g$  for both states and is independent of  $\Delta$ , which can also be seen in Figs. 2(a) and 2(b). Thus, both eigenstates show the same dynamical response to dissipation, i.e., either both are dissipation free ( $g = 0$ ) or the amplitudes decay or increase with the same rate given by  $-g$ . Although there exists a dissipation-free subspace for  $g = 0$ , and thus requirement (i) is fulfilled, requirement (ii) cannot be fulfilled simultaneously. The reason is that both states have different oscillation frequencies  $\bar{\omega} \pm \sqrt{\Delta^2 - 1}$ , and none of them is decaying, resulting in a beating pattern. We show an example of such a time evolution of the real amplitudes  $\text{Re}(a_n)$  governed by Eq. (9) in Fig. 3(a) for  $\Delta = 1.1$  and  $g = 0$ .

*c. Detailed discussion of the regime  $|\Delta| < 1$ .* After we have ruled out the possibility of synchronization [according

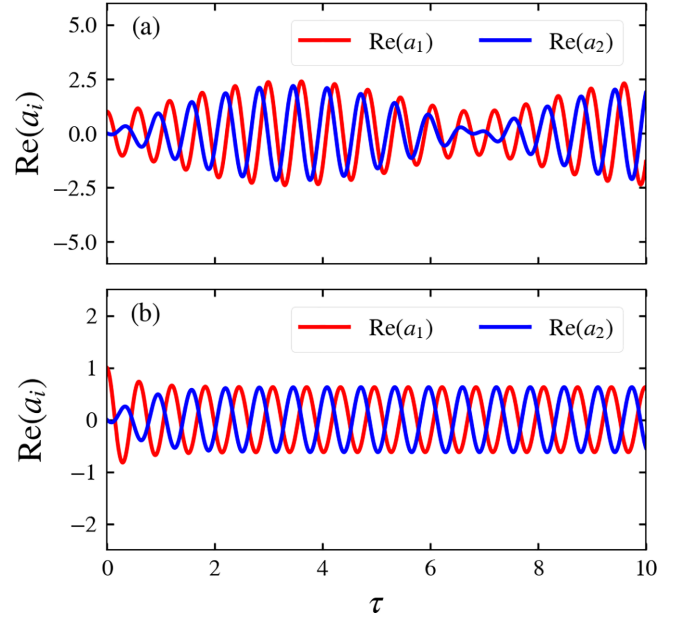


FIG. 3. Examples of different dissipation-free dynamics found for the case of  $N = 2$  oscillators. We plot the real amplitude  $\text{Re}(a_n(\tau))$  of the first oscillator in red ( $n = 1$ ) and the second one in blue ( $n = 2$ ). (a) For  $\Delta = 1.1$  and  $g = 0$ , the presence of two oscillation frequencies within the dissipation-free subspace leads to beating. (b) For  $\Delta = 0.6$  and  $g = 0.8$ , only a single eigenstate with its respective oscillation frequency is dissipation free, while the other is damped, leading to a periodic steady state of both oscillators, i.e., synchronization. Parameters:  $\bar{\omega} = 10$ ,  $\bar{a}(0) = (1, 0)^T$ . These results are obtained by direct integration of the differential equation. It agrees perfectly with the results obtained via diagonalization.

to our conditions (i)–(iii)] in the previous regime, we now discuss the case of  $|\Delta| < 1$ , where dissipation-free synchronized motion is indeed possible. For  $|\Delta| < 1$ , the eigenvalues  $\lambda_{\pm}$  are purely real [cf. Eq. (14)] and dissipation-free states are determined by  $0 = -g \pm \sqrt{1 - \Delta^2}$ , such that condition (i) may be fulfilled. In contrast to the previous case, we need to differentiate between the two states: Dissipation vanishes for the + state if  $g = g_+ \equiv \sqrt{1 - \Delta^2}$  and for the – state if  $g = g_- \equiv -\sqrt{1 - \Delta^2}$ . Each of these solutions describes a half circle with radius one, cf. Figs. 2(a) and 2(b).

We now examine whether condition (ii) is also fulfilled in this regime. When the – state is dissipation free, the amplitude of the + state is growing exponentially as  $\text{Re}(w_+(g_-)) = -g_- + \sqrt{1 - \Delta^2} = 2\sqrt{1 - \Delta^2} > 0$ . This is also verified by Fig. 2: Along the white separation in Fig. 2(a) within the regime  $|\Delta| < 1$ , the area in Fig. 2(b) is red. In contrast, along the white line in Fig. 2(b), the area in Fig. 2(a) is blue, i.e., while the + state is dissipation free, the – state is damped. Specifically,  $\text{Re}(w_-(g_+)) = -g_+ - \sqrt{1 - \Delta^2} = -2\sqrt{1 - \Delta^2} < 0$ . Thus, synchronized motion for  $|\Delta| < 1$  is found whenever the condition  $g = \sqrt{1 - \Delta^2}$  is fulfilled. Moreover, this state has a degree of synchronization of  $\mathcal{S} = 2$  and is therefore fully synchronized for all  $|\Delta| < 1$ .

In Fig. 3(b) we show the dynamics for the parameters  $\Delta = 0.6$  and  $g = 0.8$ , when starting in the initial state  $\bar{a}(0) = (1, 0)^T$ . As discussed previously, we expect to find

synchronized motion for these parameters. Indeed, after a short transient time of  $\tau \gtrsim 2$  a stationary oscillatory motion emerges where both oscillators have the same amplitude. Note the phase shift between the two oscillators, which may be understood as follows: Considering the  $+$  state  $\bar{c}_+$  [cf. Eq. (15)], the long-time dynamics is given by  $\bar{a}_{\text{sync}}(t) = \bar{c}_+ \exp(\omega_+ t)$  [cf. Eq. (7)], where  $\omega_+$  is purely imaginary. Then,

$$\text{Re}[\bar{a}_{\text{sync}}(t)] = \mathcal{N} \begin{pmatrix} \cos(i\omega_+ t + \phi) \\ \cos(i\omega_+ t) \end{pmatrix}, \quad (17)$$

where the phase difference  $\phi$  fulfills  $\tan(\phi) = -\sqrt{1 - \Delta^2}/\Delta$  and  $\mathcal{N} = (1 + |\Delta + \sqrt{\Delta^2 - 1}|^2)^{-1/2}$  is the normalization constant from Eq. (15).

## B. Many coupled oscillators on a ring

In this section, we generalize our results from the previous Sec. III A for the case of two coupled oscillators to large numbers of oscillators arranged on a ring. Also for the case of  $N$  oscillators, the dynamics is governed by Eqs. (9)–(11). In the following, we will first discuss the case of equal frequencies of all oscillators. Afterwards, we discuss the more relevant case of frequency differences.

### 1. Identical frequencies of all oscillators

To gain a basic understanding of the eigenvalue and eigenvector structure, we now consider the case when all frequencies are identical, i.e.,  $\Delta_n = \Delta$ . Then, the matrix  $W$  is circulant and its eigenvalues and (right) eigenvectors are given by [49]

$$w_j = -i(\bar{\omega} + \Delta) - \left[ g \pm 2 \cos\left(\frac{2\pi j}{N}\right) \right], \quad v \gtrsim 0, \quad (18)$$

$$\bar{c}_j = \frac{1}{\sqrt{N}} \sum_{n=1}^N e^{i\frac{2\pi}{N} j n} \bar{c}_n, \quad (19)$$

where  $\bar{c}_n$  is the  $n$ th unit vector [50]. As all eigenstates are independent of  $\Delta$  or  $g$ , one sees that most eigenvalues are doubly degenerate, i.e., there are two eigenstates with the same eigenvalue. For even  $N$  only the eigenstates with  $j = N$  and  $j = N/2$  are not degenerate; for odd  $N$  only the state with  $j = N$  is not degenerate. Moreover, the imaginary part of the eigenenergies  $w_j$ , i.e., the oscillation frequencies, is simply shifted by  $\Delta$  for all eigenstates. However, the real part of  $w_j$ , which dictates the dissipation and, more importantly, the possibility of dissipation-free dynamics, requires a more careful analysis.

*a. Positive  $v$ .* The real part of the  $j$ th eigenvalue  $\text{Re}(w_j) = 0$  if  $g = g_j \equiv -2 \cos(2\pi j/N)$ . Then all other eigenvalues  $w_{j'}$  with  $j' \neq j$  have a real part given by

$$\text{Re}(w_{j'}(g_j)) = 2 \cos\left(\frac{2\pi j}{N}\right) - 2 \cos\left(\frac{2\pi j'}{N}\right). \quad (20)$$

Furthermore, we need to distinguish the two cases of odd and even  $N$ : For an *odd* number of oscillators and  $j \neq (N \pm 1)/2$ , there is always at least one  $j'$  with  $\text{Re}(w_{j'}(g_j)) > 0$ , and thus condition (ii) is not fulfilled. On the other hand, if  $j = (N \pm 1)/2$ , then all other eigenstates are damped except for  $j' = j \mp 1$ . Yet, this state is also dissipation free and condition

(ii) cannot be fulfilled. For *even*  $N$ , however, there exists a nondegenerate eigenstate  $j = N/2$  that fulfills (i) and (ii). Then  $g = 2$  and  $\bar{c}_{\text{syn}} \equiv \bar{c}_{N/2} = \frac{1}{\sqrt{N}}(-1, 1, \dots, -1, 1)^T$ , which corresponds to anti-phase synchronization between nearest neighbors with the same frequency  $\bar{\omega} + \Delta$ .

*b. Negative  $v$ .* In contrast to the previous case, the real part of the  $j$ th eigenstate now is equal to zero if  $g = g_j \equiv +2 \cos(2\pi j/N)$ , and thus Eq. (20) becomes

$$\text{Re}(w_{j'}(g_j)) = -2 \cos\left(\frac{2\pi j}{N}\right) + 2 \cos\left(\frac{2\pi j'}{N}\right) \quad (21)$$

for all other eigenvalues  $w_{j'}$  with  $j' \neq j$ . Here, only if  $j = N$  are all other states damped and conditions (i) and (ii) fulfilled. The corresponding eigenstate is  $\bar{c}_{\text{syn}} \equiv \bar{c}_N = \frac{1}{\sqrt{N}}(1, \dots, 1)^T$ , i.e., in-phase synchronization of all oscillators with frequency  $\bar{\omega} + \Delta$ . To achieve this situation, one again has to choose  $g = 2$ .

*c. Timescales.* Let us briefly comment on the timescales on which synchronization is established. We first focus on the case where we are exactly at the dissipation-free point, characterized by  $g = 2$ . Then, the relevant timescale is the decay time of the eigenmode  $j$  with the slowest decay, i.e., the smallest value of  $|2 - 2 \cos(\frac{2\pi j}{N})|$ . Thus, the decay rate is given by  $r = |2 - 2 \cos(\frac{2\pi j}{N})|$  with corresponding timescale  $\tau \sim 1/r$ . We note that for large  $N$ , this is approximately given by  $r = 4\pi^2/N^2$ , which means that the time to reach the synchronized state increases quadratically with the number of oscillators.

Next, we investigate what happens if  $g$  is not perfectly tuned but is given by  $g = 2 + \epsilon$ . Now the synchronized state is decaying or growing with a rate  $\epsilon$ . For definiteness, we take  $\epsilon < 0$ , i.e., decaying oscillations. Importantly, the other eigenstates will decay faster than the selected one ( $j = N$  for negative  $v$  and  $j = N/2$  for positive  $v$  and even  $N$ ). The relevant decay rate of this state is now given by  $\tilde{r} = |2 + \epsilon - 2 \cos(\frac{2\pi j}{N})|$ , with corresponding timescale  $\tilde{\tau} \sim 1/\tilde{r}$ . Thus, during the time interval  $\Delta\tau = 1/|\epsilon| - \tilde{\tau}$  one can see synchronized motion.

### 2. Oscillators with different frequencies; case of small $N$

In this section, we discuss the case of arbitrary frequency differences  $\Delta_n$  for each oscillator on the ring. In this case, the matrix  $M$  [cf. Eq. (10)] can no longer be diagonalized analytically. Therefore, we discuss the basic behavior along a few examples of  $\Delta_n$  and solve the eigenvalue problem numerically. Yet, these examples demonstrate that dissipation-free synchronized motion also exists in such a general setup.

A convenient way to investigate how the properties of synchronization are affected by changes of  $\Delta_n$  is to parametrize the frequency difference according to

$$\Delta_n = s_n \Delta \quad (22)$$

and analyze the behavior of the eigenvalues and eigenvectors of  $W$  as a function of  $\Delta$  for a given (and fixed) set of  $s_n$ . Furthermore, we choose  $v$  to be *negative* such that for  $\Delta = 0$ , there exists a fully synchronized eigenstate if  $g = 2$  (see the discussion in Sec. III B 1 b). Note that a negative value of  $v$  implies  $g_j = \text{Re}(\lambda_j)$ .

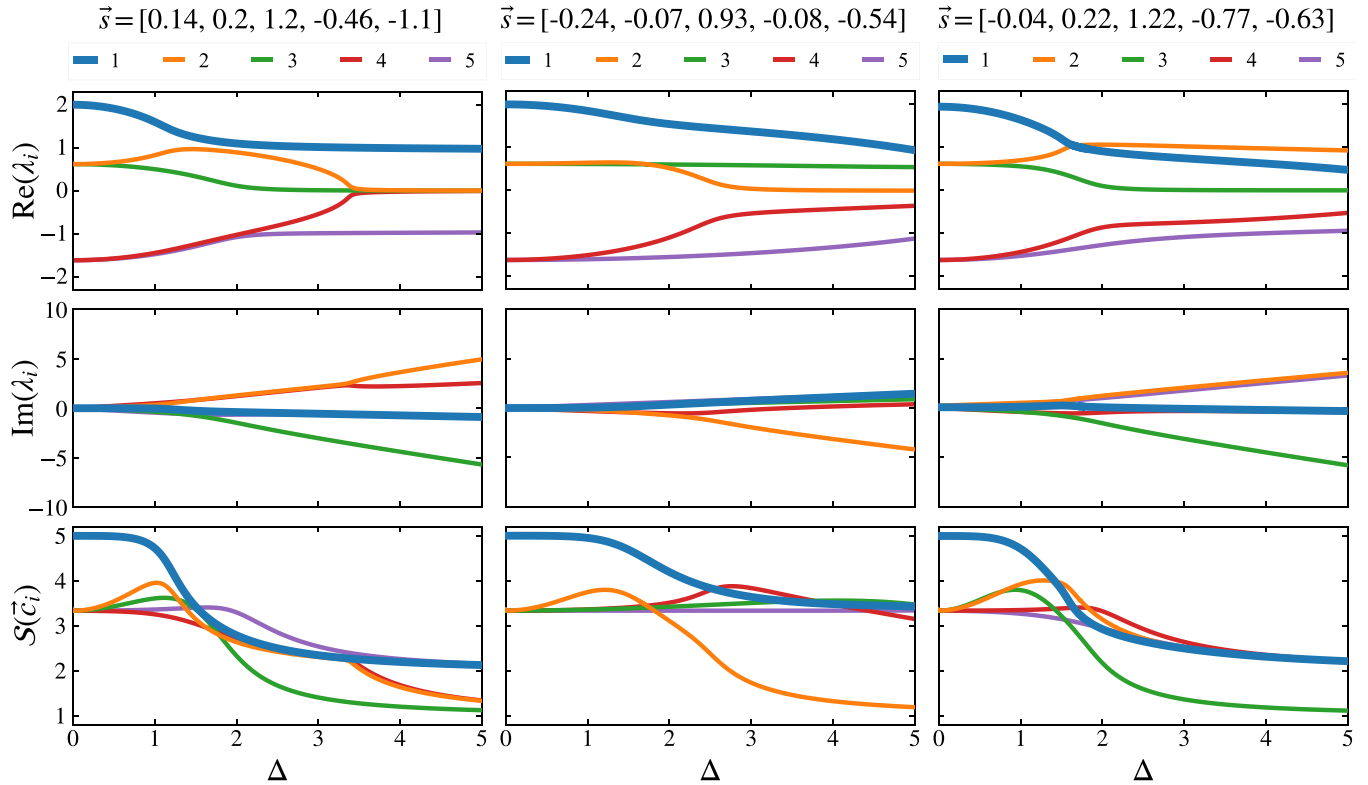


FIG. 4. Examples of dissipation-free and (fully) synchronized dynamics in a ring of  $N = 5$  oscillators with random frequency disorder. The three different columns correspond to three different set of (scaled) frequency realizations  $\vec{s}$ . The value of  $v$  is taken to be negative. In the top row we show the real part  $\text{Re}(\lambda_j)$  of the eigenvalues  $\lambda_j$  of the matrix  $M$  as a function  $\Delta$ . The middle row shows the corresponding imaginary part  $\text{Im}(\lambda_j)$  and the bottom row the degree of synchronization  $\mathcal{S}(\vec{c}_j)$  of the corresponding eigenstates  $\vec{c}_j$ . For all three considered realizations, there exists an eigenstate (blue) with the maximum value of  $\mathcal{S}$  (bottom row) for small values of  $\Delta \lesssim 1$ . This eigenstate also has the largest real part of its associated eigenvalue (top row), which allows tuning  $g$  in such a way that it becomes dissipation free while all other eigenstates are damped.

In the following we consider as an example the case of  $N = 5$  oscillators and show in Fig. 4 the results of the numerical diagonalization of the matrix  $M$  for three different realizations of  $\vec{s} = (s_1, \dots, s_5)$  (different columns). We choose the largest difference between neighboring values of  $s_n$  to be equal to 1, i.e.,  $\max(s_n - s_{n+1}) = 1$ . Then, for  $\Delta < 1$ , all frequency differences between neighboring oscillators are always smaller than the dissipative coupling between them (which has magnitude one).

The case of  $N = 2$  in our network of oscillators allows us to represent the full parameter space as shown in Fig. 2 and identify the dissipation-free subspaces and synchronization within. However, for larger system sizes (as considered now) a representation similar to Fig. 2 becomes very space consuming. Yet, a dissipation-free subspace is always necessary for synchronization, which corresponds to the white lines in Figs. 2(a) and 2(b). Thus, in order to determine whether conditions (i)–(iii) are fulfilled, it is sufficient to only search along the parameters for which each eigenstate becomes dissipation free. In particular, the relevant information of Figs. 2(a) and 2(b) may be conveniently combined to contain only  $g_{\pm} = \text{Re}(\lambda_{\pm})$  as a function of  $\Delta$ . Accordingly, the top row of Fig. 4 shows the real part of all eigenvalues  $\text{Re}(\lambda_j)$  as a function of the parameter  $\Delta$ , and the middle row shows the respective imaginary parts  $\text{Im}(\lambda_j)$ . Last, in

the bottom row, we plot the degree of synchronization  $\mathcal{S}$  of each eigenvector also as a function of  $\Delta$ . The eigenvalues of  $M$  are sorted in descending order of their real parts, i.e.,  $\text{Re}(\lambda_1) > \text{Re}(\lambda_2) > \dots > \text{Re}(\lambda_N)$ .

In the following, we discuss different regimes of  $\Delta$  and its impact on the possibility of synchronized motion in accordance with conditions (i)–(iii). We focus on the eigenstate  $\vec{c}_1$  with largest real part  $\text{Re}(\lambda_1)$  (highlighted as thick blue lines in Fig. 4). The reason is that for  $g = \text{Re}(\lambda_1)$  the eigenstate  $\vec{c}_1$  becomes dissipation free while all other eigenstates are simultaneously damped. In contrast, if we would choose  $g$  such that another eigenstate  $\vec{c}_{j \neq 1}$  would become dissipation free, then there is at least one eigenstate that is exponentially growing. It is thus sufficient to only analyze the possibility of synchronization of  $\vec{c}_1$  in the following.

*a. No frequency difference ( $\Delta = 0$ ).* This means that there are no variations in the oscillator frequencies, and the situation is exactly the same as discussed in Sec. III B 1 b. Consequently, the eigenvalues of  $W$  are given by Eq. (18). From the discussion in Sec. III B 1 b, we know that if  $g = 2 = \text{Re}(\lambda_{\text{syn}})$ , then there exists a dissipation-free synchronized state  $\vec{c}_{\text{syn}} \equiv \frac{1}{\sqrt{5}}(1, \dots, 1)^T$  with associated imaginary eigenvalue  $w_{\text{syn}} = -i\bar{\omega}$ , i.e., all oscillators are in phase and oscillate with frequency  $\bar{\omega}$ . This is exactly what we observe in Fig. 4: The eigenvalue with the largest real part has  $\text{Re}(\lambda_1) = 2$  (blue

thick lines in the top row). Note that  $\text{Re}(\lambda_2) = \text{Re}(\lambda_3)$  and  $\text{Re}(\lambda_4) = \text{Re}(\lambda_5)$ . Furthermore,  $\text{Im}(\lambda_j) = 0$  (middle row), which implies an oscillation frequency of  $\bar{\omega}$ .

*b. Small frequency differences* ( $0 < \Delta < 1$ ). In this regime, the disorder in the frequency differences between nearest-neighboring oscillators always remains smaller than the coupling between them (which is 1). We thus expect that the degree of synchronization also remains large [ $\mathcal{S}(\bar{c}_1) \approx N$ ], i.e., the full delocalization of the eigenstate  $\bar{c}_1$  persists. In the bottom row of Fig. 4, we observe exactly this behavior of the thick blue line corresponding to  $\bar{c}_1$ : For small values of  $\Delta$ ,  $\mathcal{S}(\bar{c}_1)$  is maximal and slowly decreases as  $\Delta$  approaches the value of 1. Thus, the synchronized state remains close to being fully synchronized within this regime [condition (iii)]. Note that the values for which  $\mathcal{S}(\bar{c}_1)$  starts to decrease depend on the specific realization of disorder  $\bar{s}$ .

The real part of the corresponding eigenvalue (top row) continues to be the largest value of all eigenvalues (blue thick line),  $\text{Re}(\lambda_1) > \text{Re}(\lambda_{j \neq 1})$ . Thus, for  $g = \text{Re}(\lambda_1)$  the eigenstate  $\bar{c}_1$  becomes dissipation free while all other eigenstates are damped, i.e., conditions (i) and (ii) are fulfilled. As  $\Delta$  increases,  $\text{Re}(\lambda_1)$  decreases resulting from the larger amount of frequency disorder. Simultaneously, the imaginary part  $\text{Im}(\lambda_1)$  remains close to 0 such that the oscillation frequency of the synchronized state  $\bar{c}_1$  also continues to be close to  $\bar{\omega}$ . Note, the value of  $\text{Im}(\lambda_1)$  only affects the oscillation frequency.

*c. Large frequency differences* ( $\Delta \geq 1$ ). As  $\Delta$  is increased further, the frequency difference exceeds the nearest-neighbor interaction such that—similarly to (Anderson) localization in finite systems [52]—the degree of synchronization  $\mathcal{S}(\bar{c}_1)$  of the previously delocalized eigenstate  $\bar{c}_1$  rapidly decreases as  $\Delta$  increases; see the blue thick lines in the bottom row of Fig. 4. Hence, only partial synchronization is possible in this regime, and condition (iii) is not fulfilled.

At the same time, the largest real value  $\text{Re}(\lambda_1)$  continues to decrease as a function of  $\Delta$ . Yet, close to  $\Delta = 1$ , it remains well separated from the second-largest real value  $\text{Re}(\lambda_2)$  such that a suitable choice of  $g$  still allows for dissipation-free dynamics with a single oscillation frequency. However,  $\text{Re}(\lambda_1)$  may coalesce with  $\text{Re}(\lambda_2)$  for larger values of  $\Delta$  depending on the specific realization of  $\bar{s}$ . An example of such degeneracy is observed for  $\Delta \approx 1.6$  in the top right panel of Fig. 4. As a result, both eigenstates would be dissipation free, resulting in the beating pattern discussed previously in Sec. III A. However, as mentioned above, only partial synchronization is possible in this regime anyway.

*d. Very large frequency differences* ( $\Delta \gg 1$ ). In the regime of very large frequency differences, we expect that the degree of synchronization takes its minimum value  $\mathcal{S}(\bar{c}_j) = 1$  for all eigenstates  $j$  since the scaling follows  $\Delta \gg v$ . This implies that the values  $\Delta_n = \Delta s_n$  are much larger than the dissipative coupling strength  $v$ . Then  $M$  is approximately diagonal with eigenvectors  $\bar{c}_j$  nearly localized. Note that in this limit, there is no synchronized state. We have checked numerically that for  $\Delta$  larger than the smallest difference between the  $s_n$ , the synchronization measure of all eigenstates approaches one, as expected (not shown here).

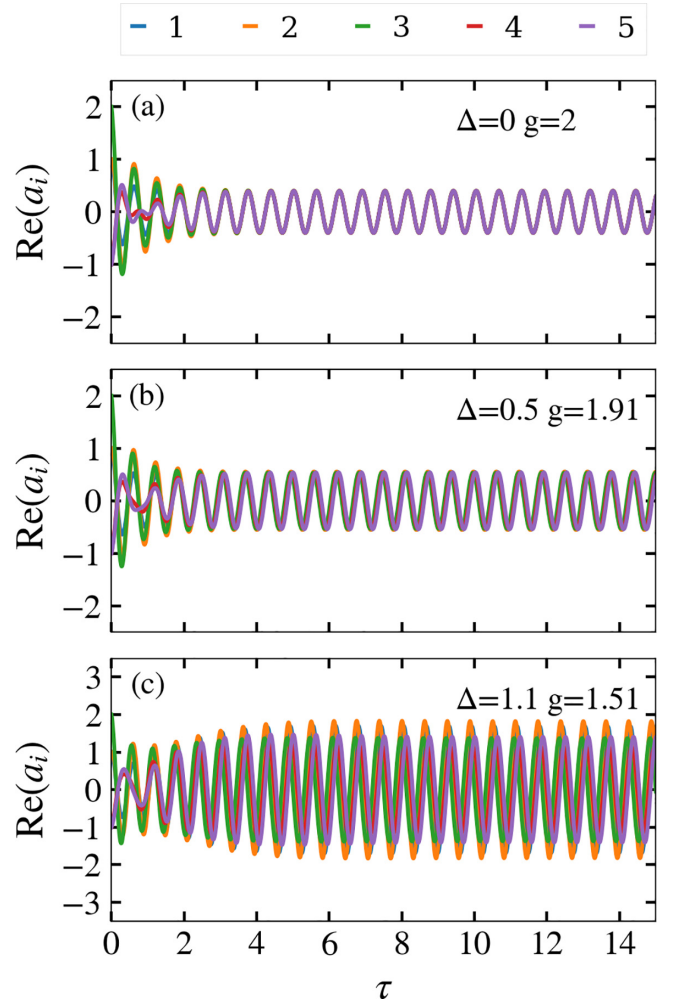


FIG. 5. Dynamical behavior of  $\text{Re}(a_i(\tau))$  given by Eq.(13) for different values of the scaling factor  $\Delta$ . In all three cases the mean frequency of the oscillators is  $\bar{\omega} = 10$  and the disorder is the same of the first panel of Fig. 4, namely  $\bar{s} = (1.14, 0.20, 1.20, -0.46, -1.1)$ . The coupling strength  $v$  is taken to be negative and all frequencies are given in units of  $|v|$ . The initial condition is  $\bar{a}_0 = (1, 1, 2, -1, -1)$ . Panels (a) and (b) show fully synchronized motion, while panel (c) is an example of partial synchronization.

Last, to demonstrate that the dynamics of the system of oscillators is consistent with our discussion of the different regimes above (obtained from analyzing the eigenvectors and eigenfrequencies), we show in Fig. 5 examples of  $\text{Re}(a_n(\tau))$  as a function of the scaled time  $\tau$  for  $\bar{s} = (1.14, 0.20, 1.20, -0.46, -1.1)$  (corresponding to the first column of Fig. 4) for three different values of  $\Delta$ . In all cases, we choose the initial state  $\bar{a}_0 = (1, 1, 2, -1, -1)^T$ .

Figure 5(a) corresponds to the case of vanishing frequency difference, i.e.,  $\Delta = 0$ . We choose the dissipation  $g = 2$  such that only the eigenstate with the largest real part is dissipation free. As expected, after a short transient time of  $\tau \approx 2.5$ , all oscillators are in-phase synchronized.

In Fig. 5(b), we increase the frequency difference to be  $\Delta = 0.5$ . Hence, the synchronized state is dissipation free for  $g = 1.91$ . Analogously to Fig. 5(a), all oscillators are

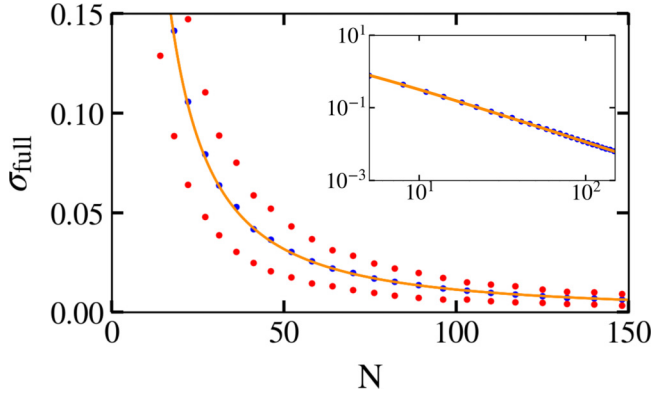


FIG. 6. Scaling of the maximal standard deviation  $\sigma_{\text{full}}$  of the distribution of  $\Delta_n$  for which one still finds full synchronization. The blue dots are the numerically obtained *mean* values of the  $\sigma_f$  distribution and the red dots are these mean values plus or minus the respective standard deviation obtained from 1000 realizations for each  $N$  (for a more detailed discussion see the main text). The orange solid line is the analytical scaling relation Eq. (23),  $\sigma_{\text{full}} = b \cdot N^{-3/2}$  with  $b = 11.5$ . The inset shows the data on a log-log scale (the red dots have been omitted for better visibility).

synchronized after a transient time of  $\tau \approx 2.5$ , yet with a small phase shift. Importantly, all oscillators have the same amplitude consistent with the finding of Fig. 4 that the degree of synchronization is maximal [ $\mathcal{S}(\bar{c}_1) = 5$  for this value of  $\Delta$ ].

Contrarily, in Fig. 5(c) where  $\Delta = 1.1$  (and  $g = 1.51$  to match the condition of dissipation-free dynamics), the amplitudes vary among the oscillators. This is in accordance with  $\mathcal{S}(\bar{c}_1) < 5$ . However, still only a single oscillation frequency is present (after some transient time). This is an example of partial synchronization.

### 3. Oscillators with different frequencies; $N$ -scaling law for total synchronization and the time interval during which synchronized motion can be observed

*a. Scaling law for full synchronization.* In the previous example, we have seen that there is an extended range of  $\Delta$  values for which there is total synchronization. In the following, we will investigate how this range changes with the number  $N$  of oscillators.

We use similar arguments as have been used to obtain scaling laws for the width of the J-band of molecular aggregates [52–54]. Note that from the definition (2), a reduction of the synchronization corresponds to localization of the eigenvector on a reduced number of oscillators. As discussed above in Sec. III B 1, for the case of identical frequencies, we found that states  $j = N$  (negative  $v$ ) and  $j = N/2$  (positive  $v$ , even  $N$ ) are the ones that lead to totally synchronized dynamics of all oscillators. Localization (i.e., a reduction of synchronization) happens when other eigenstates are mixing with this state. Such mixing happens because the fluctuations of the frequencies lead to coupling between the eigenstates defined in Eq. (19). When this coupling is comparable to the difference in eigenvalues between the eigenstates, then strong localization happens. We focus on negative  $v$ , for which the closest states to the totally delocalized one ( $j = N$ ) are the ones with  $j = N - 1$  and  $j = 1$  [55] As discussed in Sec. III B 1 c, the

corresponding difference in the values of the real parts of these states and the synchronized one scales as  $\lambda_{\text{diff}} \sim 1/N^2$  for  $N \gtrsim 10$ . Similarly to the case of a finite chain (discussed in detail in Ref. [52]) the strength of coupling between these states is  $K = \frac{1}{N} \sum_{n=1}^N \Delta_n \exp(2\pi i n/N)$  (see Appendix B for details). When each  $\Delta_n$  is chosen from a Gaussian distribution with zero mean and standard deviation  $\sigma$ , then  $K$  is also a random number with zero mean but with a scaled standard deviation of  $\tilde{\sigma}(N) = \sigma/\sqrt{N}$ . Thus, the strength of the coupling is reduced as  $1/\sqrt{N}$  with increasing  $N$ . This decrease is slower than the decrease of the difference of the eigenvalues, which scales as  $1/N^2$ . We denote by  $\sigma_{\text{full}}$  the largest standard deviation for which one still has total synchronization (for nearly all realizations of  $\Delta_n$ ). Equating  $K = \lambda_{\text{diff}}$  then gives  $\sigma_{\text{full}}/\sqrt{N} \sim 1/N^2$ , which results in the scaling

$$\sigma_{\text{full}} \sim N^{-3/2}. \quad (23)$$

This means that on increasing the number of oscillators  $N$ , the maximal width of the disorder  $\sigma_{\text{full}}$ , for which there is full synchronization, decreases as  $N^{-3/2}$ .

We have numerically verified the scaling of Eq. (23). To this end, for each  $N$  we have drawn a set of  $\Delta_n$  from independent Gaussian distribution with zero mean and standard deviation  $\sigma$  and increased  $\sigma$  until the synchronization  $\mathcal{S}$  was only a fraction  $f$  of the maximal synchronization  $\mathcal{S}_{\text{max}} = N$ , i.e.,  $\mathcal{S} = f \cdot N$ . In the example below, we have chosen  $f = 0.95$ , but choosing larger values, e.g.,  $f = 0.99$ , give the same scaling. The so obtained  $\sigma$  we denote by  $\sigma_f$ . It depends on the specific realization of  $\Delta_n$ . Repeating this procedure for many realizations one obtains for every  $N$  a distribution of  $\sigma_f$  values. In Fig. 6, the mean of 1000 realizations is plotted as blue dots. The red dots indicate the spread of the  $\sigma_f$  values (quantified via the corresponding standard deviation of the distribution of  $\sigma_f$  values). The orange curve is the analytic scaling relation of Eq. (23). We see perfect agreement between the analytical scaling and the numerically obtained values for the mean of the distribution of  $\sigma_f$ . Also, the standard deviation of the  $\sigma_f$  distribution decreases with the same scaling. Note that in the analytic description, we have  $\sigma_{\text{full}} = b \cdot N^{-3/2}$ , with a prefactor  $b$  that depends on the specific criterium of “localized.” Similarly, in the numerical case the values of  $\sigma_f$  depend on the choice of  $f$ . Therefore, in Fig. 6, we have adjusted this prefactor  $b$  for the orange curve.

*b. Locating the dissipation-free space and the time interval of synchronized motion.* As we have seen from the discussion above, sufficiently small fluctuations of  $\Delta_n$  do not pose a problem to achieve a large synchronization measure. For the case of a small number of oscillators ( $N \sim 5$ ) we have explicitly shown examples for specific choices of the realizations of  $\Delta_n$ . We now investigate shifts of the real part of  $\lambda$  caused by  $\Delta_n$ . Such shifts imply, on the one hand, that for each realization of  $\Delta_n$ , one has a different value of  $g$  in order to be in the dissipation-free subspace. On the other hand, the timescale on which the synchronized state is reached is also affected. In the following, we focus on the regime where full synchronization is obtained. We also restrict the discussion to the case of negative  $v$ , where the synchronized state in the case of no disorder is characterized by  $j = N$ . As discussed in Sec. III B 1 c, the

relevant timescale  $\tilde{\tau}$  in which the synchronized state is reached is given by  $1/\tilde{\tau} = \tilde{r} = |g - \text{Re}(\lambda_{\tilde{j}})|$ , where  $\tilde{j}$  labels the state that has a real part that is closest to that of the synchronized state (in the disorder-free case we have  $\tilde{j} = 1$  and  $\tilde{j} = N - 1$ ). We now consider the case when  $\Delta_n$  are randomly distributed according to independent identical Gaussian distributions for each oscillator with zero mean and standard deviation  $\sigma$ . For sufficiently small disorder, we find analytically (see Appendix B) and numerically that the average value (denoted by  $\langle \cdot \rangle$ ) of the real part of the synchronized state is reduced by  $|\text{Re}(\langle \Delta \lambda_{\text{sync}} \rangle)| \approx \frac{N}{12} \sigma^2$  with respect to the disorder-free value  $\text{Re}(\lambda_N) = 2$ , i.e.,  $\text{Re}(\langle \lambda_{\text{sync}} \rangle) = 2 - \frac{N}{12} \sigma^2$ . This holds when  $\sigma$  is so small that one is in the fully synchronized regime. For definiteness, we discuss in the following the case  $g = 2$ , i.e., the value according to the disorder-free case. Then one can show that for all individual realizations this state is damped, and the average decay is  $\tau_{\text{sync}} \approx \frac{12}{N\sigma^2}$ . The disorder also influences the timescale  $\tilde{\tau}$  on which the synchronized state is reached. We find (see Appendix B) that for  $g = 2$  and  $N$  larger than 20, one has  $\tilde{\tau} \approx |\frac{4\pi^2}{N^2}|^{-1} = \frac{1}{4\pi^2} N^2$ , which is independent of  $\sigma$ . With this, one finds the time during which synchronized motion can be seen  $\Delta\tau = \tau_{\text{sync}} - \tilde{\tau} \approx \tau_{\text{sync}} \approx \frac{12}{N\sigma^2}$ . Note that this holds for  $\sigma \lesssim 10 \cdot N^{-3/2}$ .

This expression is derived using the individual mean values  $\langle \lambda_j \rangle$  to calculate the time interval according to  $\Delta\tau = \frac{1}{|\text{Re}(w_N)|} - \frac{1}{|\text{Re}(w_{1,\pm})|}$ . In a numerical test, we have also considered the more accurate expression  $\Delta\tau = \langle \frac{1}{|\text{Re}(w_N)|} - \frac{1}{|\text{Re}(w_{1,\pm})|} \rangle$ , i.e., the average of the observable time of synchronization for each realization. We found that both considerations result in basically the same estimates of the synchronization time, namely  $\Delta\tau \approx \frac{12}{N\sigma^2}$ , where as above  $\sigma \lesssim 10 \cdot N^{-3/2}$ .

#### IV. CONCLUSIONS

In this work we have investigated the possibility of long-lived synchronized motion in a ring of harmonic oscillators, which are subject to gain or loss and interact via nearest-neighbor dissipative couplings. In this context, we refer to synchronization as the existence of a single eigenstate of the dynamical matrix, which is dissipation free. Furthermore, if it attains the maximum value of the (inverse) participation ratio, then we refer to it as “fully synchronized.” We find that in the case of only two coupled oscillators, synchronization may always be achieved by tuning the gain appropriately as long as the frequency difference between the two oscillators is smaller than their interaction strength.

Similar behavior is observed in larger networks, i.e., many oscillators arranged on a ring with nearest-neighbor interactions, yet the possibility of synchronization then depends on the specifics of the system at hand: If all oscillators are identical, then synchronized collective motion may be achieved for an even number of sites with repulsive dissipative couplings ( $v$  positive) or an odd number of sites with attractive dissipative interactions ( $v$  negative). For small frequency differences compared to the coupling between the oscillators, this behavior remains, which we show specifically for the case of  $N = 5$ . If all frequency differences between

neighboring oscillators are much smaller than their coupling, then one still has synchronized motion. For larger frequency differences, the synchronization decreases quickly with increasing differences. This is similar to Anderson localization [53] in tight-binding Hamiltonians with *real* matrix elements and on-site disorder. We note that in the present case with a non-Hermitian Hamiltonian, we observe a different behavior for the real and imaginary parts; in particular, we observe “localization” in the real part but not the imaginary part.

For a larger number  $N$  of oscillators, we use the standard deviation  $\sigma$  of the frequency variations of the oscillators to quantify their inhomogeneity. We find that the range of  $\sigma$  values for which there is full synchronization scales as  $N^{-3/2}$ . This means that for a larger number of oscillators, the range of  $\sigma$  values that give full synchronization is strongly reduced. For example, for  $N \approx 100$ , one has full synchronization for  $\sigma$  smaller than approximately 1% of the interaction.

Synchronization, as discussed in this work, is intimately related to the existence of dissipation-free dynamics and, thus, isolated points or submanifolds in parameter space. Hence, they require a very precise tuning of gain and loss in order to obtain periodic steady states. This is, however, hard to achieve in any realistic experiment, and the synchronized state will experience some gain or loss. We can relax the condition  $\text{Re}(w_j) = 0$  by solely requiring  $|\text{Re}(w_j)| \ll |\text{Im}(w_j)|$ , which means that the change of amplitude of oscillation is small over many oscillations. In addition, we then require  $\text{Re}(w_j) \ll \text{Re}(w_{\text{sync}})$ , which means that all other eigenstates decay much faster than the “synchronized” one. In principle, one may relax the condition even further and demand that there exists only one state with  $\text{Re}(w_j) > 0$ , while all other states fulfill  $\text{Re}(w_i) \leq 0$ . Then, the synchronized state would grow while all other states are exponentially damped.

For the case of disorder in the oscillator frequencies and gain and loss chosen according to the disorder-free case, we have investigated the time interval during which synchronized motion can be observed. For this case, all the eigenstates are exponentially damped. We find that for  $\sigma \lesssim N^{-3/2}$  the time during which synchronization can be observed scales as  $\Delta\tau \approx \tau_{\text{sync}} \approx \frac{12}{N\sigma^2}$ .

Finally, we want to comment on the role of the connectivity of the oscillators. In the present work, the oscillators are in a ring arrangement, with nearest-neighbor interactions and equal interactions. The results obtained are specific for this arrangement. For example, if one removes one interaction (“linear chain”), then one sees that the maximum synchronization is  $\frac{2}{3}N$ . Apart from this we expect that such a configuration shows very similar scaling behavior as the ring. However, in general, every configuration has its specific maximal synchronization and its specific scaling laws. Such a sensitivity of the system’s dynamical properties to the network topology has been studied recently in the context of Kuramoto oscillators [56]. Thus, also for linear oscillator models, every arrangement needs a new analysis.

#### ACKNOWLEDGMENTS

C.W.W. acknowledges support from the Max-Planck Gesellschaft via the MPI-PKS Next Step fellowship and is financially supported by the Deutsche Forschungsgemeinschaft

(DFG, German Research Foundation) Project No. 496502542 (WA 5170/1-1). A.E. acknowledges support from the DFG via a Heisenberg fellowship (Grant No. EI 872/10-1).

## APPENDIX A: DIFFERENT REPRESENTATIONS OF THE EQUATIONS OF MOTION

Here we provide different representations of Eq. (3).

### 1. Separation in real and imaginary parts

Introducing  $a_n = x_n + ip_n$  and  $W_{nm} = W_{nm}^R + iW_{nm}^I$  in Eq. (3) gives

$$\dot{x}_n + i\dot{p}_n = \sum_m (W_{nm}^R + iW_{nm}^I)(x_m + ip_m). \quad (\text{A1})$$

Or written explicitly as a linear system of coupled equation for the real and imaginary parts,

$$\dot{x}_n = \sum_m (W_{nm}^R x_m - W_{nm}^I p_m), \quad (\text{A2})$$

$$\dot{p}_n = \sum_m (W_{nm}^R p_m + W_{nm}^I x_m). \quad (\text{A3})$$

### 2. Representation with real amplitude and phase

Introducing  $a_n = r_n e^{i\phi_n}$  with real  $r_n$  and real  $\phi_n$  allows one to write Eq. (3) as

$$\frac{d}{dt}(r_n e^{i\phi_n}) = \sum_m W_{nm} r_m e^{i\phi_m}. \quad (\text{A4})$$

Note that both  $r_n$  and real  $\phi_n$  depend on time.

## APPENDIX B: SCALING LAWS

In this Appendix we provide the main steps to derive the scaling laws of Sec. III B 3.

### 1. Perturbation theory for disorder in the frequencies

We write Eq. (10) as  $M = M_0 + M'$ , where  $M_0 = M(\{\Delta_n = 0\})$  is the matrix  $M$  with all  $\Delta_n = 0$  and  $M' = -i \text{diag}[\Delta_1, \dots, \Delta_N]$  is the diagonal matrix with the elements  $-i\Delta_n$  on the diagonal. Using the eigenbasis of  $M_0$  we can write Eq. (10) as

$$M = \sum_\ell \lambda_\ell \bar{v}_\ell \bar{v}_\ell^\dagger + \sum_\ell \sum_{\ell'} \bar{v}_\ell K_{\ell, \ell'} \bar{v}_{\ell'}^\dagger \quad (\text{B1})$$

with the matrix elements of the matrix  $K$  given by

$$K_{\ell, \ell'} = -\frac{i}{N} \sum_{n=1}^N \Delta_n e^{2\pi i(\ell - \ell')n/N}. \quad (\text{B2})$$

Note that  $K$  is anti-Hermitian and therefore  $K_{ij}^* \neq K_{ji}$ . It is convenient to introduce a corresponding Hermitian operator,

$$K^H = iK. \quad (\text{B3})$$

Note also that  $\bar{v}_\ell^\dagger \bar{v}_{\ell'} = \delta_{\ell\ell'}$ .

We consider the case  $v < 0$ . Then the matrix  $M$  reads [cf. Eq. (10)]

$$M = \begin{pmatrix} -i\Delta_1 & 1 & 0 & \dots & 1 \\ 1 & -i\Delta_2 & 1 & \dots & 0 \\ 0 & 1 & & & \\ \vdots & & & & \\ 1 & 0 & \dots & 1 & -i\Delta_N \end{pmatrix} \quad (\text{B4})$$

and the eigenvalues of the matrix  $M_0$  are

$$\lambda_\ell = 2 \cos(2\pi\ell/N). \quad (\text{B5})$$

#### a. Corrections to the state $j = N$

The first-order correction to the state  $j = N$  is

$$K_N^{(1)} = \bar{v}_N^\dagger K \bar{v}_N = -iK_{N,N}^H = -\frac{i}{N} \sum_{n=1}^N \Delta_n. \quad (\text{B6})$$

When the  $\Delta_n$  are independent Gaussian random variables with mean zero and standard deviation  $\sigma$ , then  $K_N^{(1)}$  is also a Gaussian random variable with zero mean but standard deviation  $\sigma/\sqrt{N}$ . Note that  $K_N^{(1)}$  is purely imaginary. Since we are primarily interested in the decay times, which are related to the real part of the eigenvalues of  $M$ , we need to evaluate the second-order correction,

$$\begin{aligned} K_N^{(2)} &= -\sum_{\ell \neq N} \frac{(v_\ell^\dagger K^H v_N)(v_N^\dagger K^H v_\ell)}{\lambda_N - \lambda_\ell} \\ &= -\frac{1}{N^2} \sum_{n=1}^N \sum_{m=1}^N \Delta_n \Delta_m \sum_{\ell \neq N} \frac{e^{i2\pi\ell(n-m)/N}}{2 - 2\cos(2\pi\ell/N)}. \end{aligned} \quad (\text{B7})$$

This quantity is purely real.

Calculating the mean over a disorder distribution for uncorrelated fluctuations of the  $\Delta_n$  we find using  $\langle \Delta_n \Delta_m \rangle = \delta_{nm}$ ,

$$\langle K_N^{(2)} \rangle = -\frac{1}{N^2} \sum_{\ell \neq N} \frac{1}{2 - 2\cos(2\pi\ell/N)} \sum_{n=1}^N \langle \Delta_n^2 \rangle. \quad (\text{B8})$$

The sum over  $\ell$  can be calculated explicitly,

$$\begin{aligned} \frac{-1}{N^2} \sum_{\ell \neq N} \frac{1}{2 - 2\cos(2\pi\ell/N)} &= \frac{1}{12} \frac{-N^2 + 1}{N^2} \\ &= \frac{1}{12} \left( -1 + \frac{1}{N^2} \right), \end{aligned} \quad (\text{B9})$$

such that we arrive at

$$\langle K_N^{(2)} \rangle = \frac{1}{12} \left( -1 + \frac{1}{N^2} \right) \sum_{n=1}^N \langle \Delta_n^2 \rangle. \quad (\text{B10})$$

Taking all  $\langle \Delta_n^2 \rangle \equiv \sigma^2$  to be identical and choosing  $\langle \Delta_n \rangle = 0$  we have  $K^{(2)} \approx -\frac{1}{12} N \sigma^2$ . The second-order correction to the state  $j = N$  is  $\lambda_N^{(2)} = \lambda_N + K^{(1)} + K^{(2)}$ . For the real part we then obtain

$$\text{Re}(\lambda_N^{(2)}(\sigma)) \approx 2 - \frac{1}{12} N \sigma^2. \quad (\text{B11})$$

#### b. Corrections to the degenerate states $j = N - 1$ and $j = 1$

For  $v < 0$ , i.e., the case we consider here, the two states  $j = N - 1$  and  $j = 1$  are degenerate, with eigenvalue  $\lambda_1 =$

$\lambda_{N-1} = 2 \cos(2\pi/N)$ . The coupling elements between these two states are

$$K_{1,N-1} = -\frac{i}{N} \sum_n \Delta_n e^{4\pi i n/N} \equiv -ir e^{i\phi}, \quad (\text{B12})$$

$$K_{N-1,1} = -\frac{i}{N} \sum_n \Delta_n e^{-4\pi i n/N} = -ir e^{-i\phi}, \quad (\text{B13})$$

where  $r = |K_{1,N-1}|$  and  $\phi$  is the corresponding phase. Both quantities depend on  $\Delta_n$ . Diagonalizing this degenerate subspace gives the new zeroth-order states,

$$\bar{v}_\pm = \frac{1}{\sqrt{2}}(e^{i\phi} \bar{v}_1 \pm \bar{v}_{N-1}) \quad \lambda_\pm = \lambda_1 \mp i|K_{1,N-1}^H|. \quad (\text{B14})$$

The correction to the eigenvalues is purely imaginary. Since we are interested in the real part, we perform perturbation theory with the states  $\bar{v}_\pm$  and  $\bar{v}_j$  with  $j \neq 1, N-1$ . The second-order corrections to the degenerate states are given by

$$\begin{aligned} K_{1,\pm}^{(2)} &= \sum_{j \neq \pm} \frac{(\bar{v}_j^\dagger K \bar{v}_\pm)(\bar{v}_\pm^\dagger K \bar{v}_j)}{\lambda_\pm - \lambda_j} \\ &= \sum_{j \neq \pm} \frac{K_{j,1} K_{1,j} + K_{j,N-1} K_{N-1,j}}{2(\lambda_\pm - \lambda_j)} \\ &\quad \pm \sum_{j \neq \pm} \frac{[e^{i\phi} K_{j,1} K_{N-1,j}]}{2(\lambda_\pm - \lambda_j)} \pm \sum_{j \neq \pm} \frac{[e^{-i\phi} K_{j,N-1} K_{1,j}]}{2(\lambda_\pm - \lambda_j)}. \end{aligned} \quad (\text{B15})$$

Using the definition (B3),  $K_{1,\pm}^{(2)}$  may be expressed as

$$\begin{aligned} K_{1,\pm}^{(2)} &= - \sum_{j \neq \pm} \frac{|K_{j,1}^H|^2 + |K_{j,N-1}^H|^2}{2(\lambda_\pm - \lambda_j)} \mp \sum_{j \neq \pm} \frac{[e^{i\phi} K_{j,1}^H K_{N-1,j}^H]}{2(\lambda_\pm - \lambda_j)} \\ &\quad \mp \sum_{j \neq \pm} \frac{[e^{-i\phi} (K_{N-1,j}^H)^* (K_{j,1}^H)^*]}{2(\lambda_\pm - \lambda_j)}. \end{aligned} \quad (\text{B16})$$

Then the eigenvalues including the second-order correction are given by

$$\begin{aligned} \lambda_{1,\pm}^{(2)} &= \lambda_1 \mp i|K_{1,N-1}^H| \\ &\quad - \sum_{j \neq \pm} \frac{|K_{j,1}^H|^2 + |K_{j,N-1}^H|^2 \pm 2\text{Re}[e^{i\phi} K_{j,1}^H K_{N-1,j}^H]}{2(\lambda_\pm - \lambda_j)}. \end{aligned} \quad (\text{B17})$$

Note that  $K_{j,i}^H$ ,  $\phi$ , and  $\lambda_\pm$  depend on all  $\Delta_n$ . We found that, on averaging, the term containing the phase  $\phi$  is always small compared to the other terms such that we neglect it in the

following. For the mean of the real part we then obtain

$$\begin{aligned} \text{Re}\langle \lambda_{1,\pm}^{(2)} \rangle &= \lambda_1 - \sum_{j \neq \pm} \text{Re} \left\langle \frac{|K_{j,1}^H|^2 + |K_{j,N-1}^H|^2}{2(\lambda_1 - \lambda_j) \mp i|K_{1,N-1}^H|} \right\rangle, \quad (\text{B18}) \\ &= \lambda_1 - 2 \sum_{j \neq \pm} (\lambda_1 - \lambda_j) \left\langle \frac{|K_{j,1}^H|^2 + |K_{j,N-1}^H|^2}{4(\lambda_1 - \lambda_j)^2 + |K_{1,N-1}^H|^2} \right\rangle. \end{aligned} \quad (\text{B19})$$

To evaluate the average, we approximate  $|K_{1,N-1}^H|^2$  in the denominator by its average and obtain

$$\text{Re}\langle \lambda_{1,\pm}^{(2)} \rangle = \lambda_1 - 2 \sum_{j \neq \pm} (\lambda_1 - \lambda_j) \frac{\langle |K_{j,1}^H|^2 \rangle + \langle |K_{j,N-1}^H|^2 \rangle}{4(\lambda_1 - \lambda_j)^2 + \langle |K_{1,N-1}^H|^2 \rangle}. \quad (\text{B20})$$

We may now evaluate the expectation values. It holds [cf. Eq. (B2)]

$$\langle |K_{j,j'}^H|^2 \rangle = \frac{1}{N^2} \sum_{n=1}^N \sum_{m=1}^N e^{\frac{2\pi i(j-j')(n-m)}{N}} \langle \Delta_n \Delta_m \rangle, \quad (\text{B21})$$

$$= \frac{1}{N^2} \sum_{n=1}^N \langle \Delta_n^2 \rangle. \quad (\text{B22})$$

The second line follows from the fact that different  $\Delta_n$  are statistically independent. Assuming that the variance is equal for all  $\Delta_n$ , i.e.,  $\langle \Delta_n^2 \rangle = \sigma^2$ , we obtain

$$\text{Re}\langle \lambda_{1,\pm}^{(2)} \rangle \approx \lambda_1 - 2 \sum_{j \neq \pm} (\lambda_1 - \lambda_j) \frac{\sigma^2/N + \sigma^2/N}{4(\lambda_1 - \lambda_j)^2 + \sigma^2/N}. \quad (\text{B23})$$

Note that the condition  $j \neq \pm$  is equivalent to  $j \neq 1, N-1$ . The smallest difference is given by  $\lambda_1 - \lambda_2 \approx 12\pi^2/N^2$ . Furthermore, since in the above derivation we assume that one is in the fully synchronized regime,  $\sigma$  has to be sufficiently small. This requires  $\sigma \sim N^{-3/2}$  as discussed in the main text. Then, we can safely neglect the term  $\sigma^2/N$  in the denominator and obtain

$$\text{Re}\langle \lambda_{1,\pm}^{(2)} \rangle \approx \lambda_1 - \sum_{j \neq \pm} \frac{1}{N|\lambda_1 - \lambda_j|} \sigma^2. \quad (\text{B24})$$

We have  $\lambda_1 = 2 \cos(2\pi/N) \approx 2 - 4\pi^2/N^2$ . It turns out that for values of  $\sigma$  such that one is in the fully synchronized regime the second term in Eq. (B24) is small compared to  $4\pi^2/N^2$  and can be neglected, so that one finally obtains

$$\text{Re}\langle \lambda_{1,\pm}^{(2)} \rangle \approx 2 - 4\pi^2/N^2. \quad (\text{B25})$$

The timescale on which the synchronized state is reached is thus  $\tilde{\tau} \approx 1/|g - 2 + 4\pi^2/N^2|$ . We compared these analytical estimates with results obtained by full numerical diagonalization of the matrix  $W$  and averaging over realizations of the  $\Delta_n$ . We found nearly perfect agreement.

[1] A. Pikovsky, J. Kurths, M. Rosenblum, and J. Kurths, *Synchronization: A Universal Concept in Nonlinear Sciences* (Cambridge University Press, Cambridge, UK, 2003).

[2] S. H. Strogatz, *Nonlinear Dynamics and Chaos: With Applications to Physics, Biology, Chemistry, and Engineering* (CRC Press, Boca Raton, FL, 2018).

- [3] M. Bennett, M. F. Schatz, H. Rockwood, and K. Wiesenfeld, *Proc. R. Soc. Lond. A* **458**, 563 (2002).
- [4] S. H. Strogatz and I. Stewart, *Sci. Am.* **269**, 102 (1993).
- [5] M. Rosenblum and A. Pikovsky, *Contemp. Phys.* **44**, 401 (2003).
- [6] A. Arenas, A. Díaz-Guilera, J. Kurths, Y. Moreno, and C. Zhou, *Phys. Rep.* **469**, 93 (2008).
- [7] K. S. Thornburg, M. Möller, R. Roy, T. W. Carr, R.-D. Li, and T. Erneux, *Phys. Rev. E* **55**, 3865 (1997).
- [8] J. J. Lynch and R. A. York, *IEEE Microw. Guid. Wave Lett.* **5**, 213 (1995).
- [9] A. B. Cawthorne, P. Barbara, S. V. Shitov, C. J. Lobb, K. Wiesenfeld, and A. Zangwill, *Phys. Rev. B* **60**, 7575 (1999).
- [10] R. Fazio and H. Van Der Zant, *Phys. Rep.* **355**, 235 (2001).
- [11] A. Slavín, *Nat. Nanotechnol.* **4**, 479 (2009).
- [12] T. Nishikawa and A. E. Motter, *New J. Phys.* **17**, 015012 (2015).
- [13] J. C. Bellamy, *IEEE Commun. Mag.* **33**, 70 (1995).
- [14] L. Narula and T. E. Humphreys, *IEEE J. Sel. Top. Sign. Process.* **12**, 749 (2018).
- [15] A. Jenkins, *Phys. Rep.* **525**, 167 (2013).
- [16] L. Muller, J. Mináč, and T. T. Nguyen, *Phys. Rev. E* **104**, L022201 (2021).
- [17] W. Ren, *Automatica* **44**, 3195 (2008).
- [18] L. Scardovi and R. Sepulchre, *Automatica* **45**, 2557 (2009).
- [19] Y. Yang, W. He, and Q.-L. Han, *IEEE Trans. Circ. Syst. I: Regul. Pap.* **68**, 2148 (2021).
- [20] Y. Yang, C. Peng, and Q.-L. Han, *IEEE Trans. Syst. Man Cybernet.: Syst.* **53**, 789 (2023).
- [21] C. Desoer, *IRE Trans. Circ. Theory* **7**, 211 (1960).
- [22] K. J. Vahala, *Nature (London)* **424**, 839846 (2003).
- [23] R. El-Ganainy, A. Einfeld, M. Levy, and D. N. Christodoulides, *Appl. Phys. Lett.* **103**, 161105 (2013).
- [24] K. Okamoto (ed.), *Fundamentals of Optical Waveguides (Third Edition)*, (Academic Press, San Diego, CA, 2022), p. iv.
- [25] J. S. Briggs and A. Einfeld, *Phys. Rev. A* **85**, 052111 (2012).
- [26] H. Goldstein, C. Poole, and J. Safko, *Classical Mechanics* (Addison-Wesley, New York, 2002).
- [27] W. Greiner and D. A. Bromley, *Classical Mechanics: Systems of Particles and Hamiltonian Dynamics* (Springer, Berlin, 2003).
- [28] H. P. Breuer and F. Petruccione, *The Theory of Open Quantum Systems* (Oxford University Press, Oxford, 2002).
- [29] D. H. Zanette, *J. Phys. Commun.* **2**, 095015 (2018).
- [30] J. Rohn, K. P. Schmidt, and C. Genes, [arXiv:2111.02201](https://arxiv.org/abs/2111.02201).
- [31] J. Ding, I. Belykh, A. Marandi, and M.-A. Miri, *Phys. Rev. Appl.* **12**, 054039 (2019).
- [32] D. Mukhopadhyay, J. M. P. Nair, and G. S. Agarwal, *Phys. Rev. B* **105**, 064405 (2022).
- [33] S. R. Mbokop Tchounda, P. Djorwé, S. G. Nana Engo, and B. Djafari-Rouhani, *Phys. Rev. Appl.* **19**, 064016 (2023).
- [34] F. Yang, Y.-C. Liu, and L. You, *Phys. Rev. A* **96**, 053845 (2017).
- [35] A. Metelmann and A. A. Clerk, *Phys. Rev. X* **5**, 021025 (2015).
- [36] F.-J. Shu, C.-L. Zou, X.-B. Zou, and L. Yang, *Phys. Rev. A* **94**, 013848 (2016).
- [37] J. M. P. Nair, D. Mukhopadhyay, and G. S. Agarwal, *Phys. Rev. Lett.* **126**, 180401 (2021).
- [38] M. Honari-Latifpour and M.-A. Miri, *Phys. Rev. Res.* **2**, 043335 (2020).
- [39] A. Tomadin, V. Giovannetti, R. Fazio, D. Gerace, I. Carusotto, H. E. Türeci, and A. Imamoglu, *Phys. Rev. A* **81**, 061801(R) (2010).
- [40] B. Kramer and A. MacKinnon, *Rep. Prog. Phys.* **56**, 1469 (1993).
- [41] M. H. Teimourpour, R. El-Ganainy, A. Einfeld, A. Szameit, and D. N. Christodoulides, *Phys. Rev. A* **90**, 053817 (2014).
- [42] S. Yan, Y. Mao, J. Xu, H. Ji, W. Liu, J. Ma, X. Long, X. Xu, Z. Tan, and C. Zhang, *Opt. Commun.* **546**, 129760 (2023).
- [43] C. M. Bender, M. V. Berry, and A. Mandilara, *J. Phys. A* **35**, L467 (2002).
- [44] V. V. Konotop, J. Yang, and D. A. Zezyulin, *Rev. Mod. Phys.* **88**, 035002 (2016).
- [45] M. Müller and I. Rotter, *J. Phys. A: Math. Theor.* **41**, 244018 (2008).
- [46] W. D. Heiss, *J. Phys. A: Math. Theor.* **45**, 444016 (2012).
- [47] R. El-Ganainy, K. G. Makris, M. Khajavikhan, Z. H. Musslimani, S. Rotter, and D. N. Christodoulides, *Nat. Phys.* **14**, 11 (2018).
- [48] M.-A. Miri and A. AlĀ<sup>1</sup>, *Science* **363**, eaar7709 (2019).
- [49] R. M. Gray, *FNT Commun. Inf. Theory* **2**, 155 (2005).
- [50] We remark that the eigenenergies and eigenvectors Eq. (18) and Eq. (19) are very different from the ones of a fully connected network of oscillators with equal couplings between all oscillators as it appears for example in the linear representation of the Kuramoto model [51].
- [51] D. C. Roberts, *Phys. Rev. E* **77**, 031114 (2008).
- [52] S. Möbius, S. Vlaming, V. Malyshev, J. Knoester, and A. Einfeld, [arXiv:1404.4475](https://arxiv.org/abs/1404.4475).
- [53] V. A. Malyshev, *J. Lumin.* **55**, 225 (1993).
- [54] A. Einfeld, S. M. Vlaming, V. A. Malyshev, and J. Knoester, *Phys. Rev. Lett.* **105**, 137402 (2010).
- [55] For positive  $v$  the delocalized state is  $j = N/2$  the “closest” states are  $j = N/2 \pm 1$ .
- [56] K. L. Rossi, R. C. Budzinski, B. R. R. Boaretto, L. E. Muller, and U. Feudel, *Phys. Rev. Res.* **5**, 013220 (2023).